Ultrafast Spectral Dynamics of $CsPb(Br_xCl_{1-x})_3$ Mixed-Halide Nanocrystals

Naiya Soetan,[a] Alexander Puretzky,[b] Kemar Reid,[c] Abdelaziz Boulesbaa,[b] Holly F. Zarick,[a] Andrew Hunt,[a] Olivia Rose,[a] Sandra Rosenthal,[c, d] David B. Geohegan,[b] and Rizia Bardhan[a*]

[a]Department of Chemical and Biomolecular Engineering & [c]Department of Interdisciplinary Materials Science, Vanderbilt University, Nashville, TN 37235, USA. [b]Center for Nanophase Materials Sciences, Oak Ridge National Laboratory, Oak Ridge, TN 37831, USA

E-mail: rizia.bardhan@vanderbilt.edu

Table S1: EDS data of mixed halide samples. The values given are atomic percent. Note that the Cl content refers to the percentage of the halide component that is Cl.

Cl content	**% Cesium**	**% Bromine**	**% Chlorine**	**% Lead**
16%	21.4	47.2	8.8	22.6
22%	19.9	46.3	13.0	20.8
45%	19.9	32.3	26.9	20.9

From EDS we calculated Cl content the following way:
Cl content = %Chlorine/(%Chlorine + %Bromine)

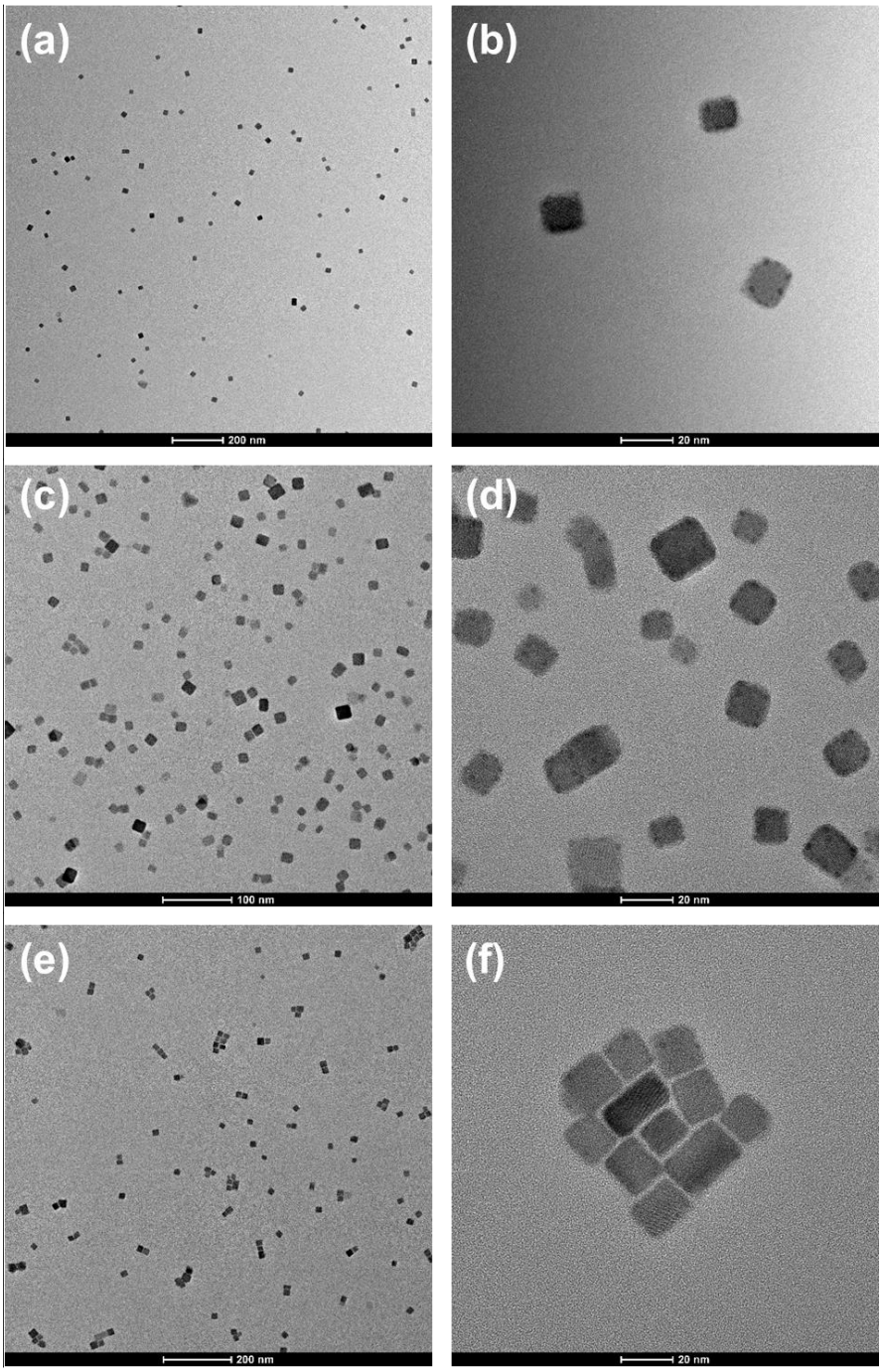

Figure S1: TEM images of (a-b) $CsPbBr_3$, (c,d) $CsPb(Br_{0.84}Cl_{0.16})_3$, and (e,f) $CsPb(Br_{0.55}Cl_{0.45})_3$ perovskite NCs.

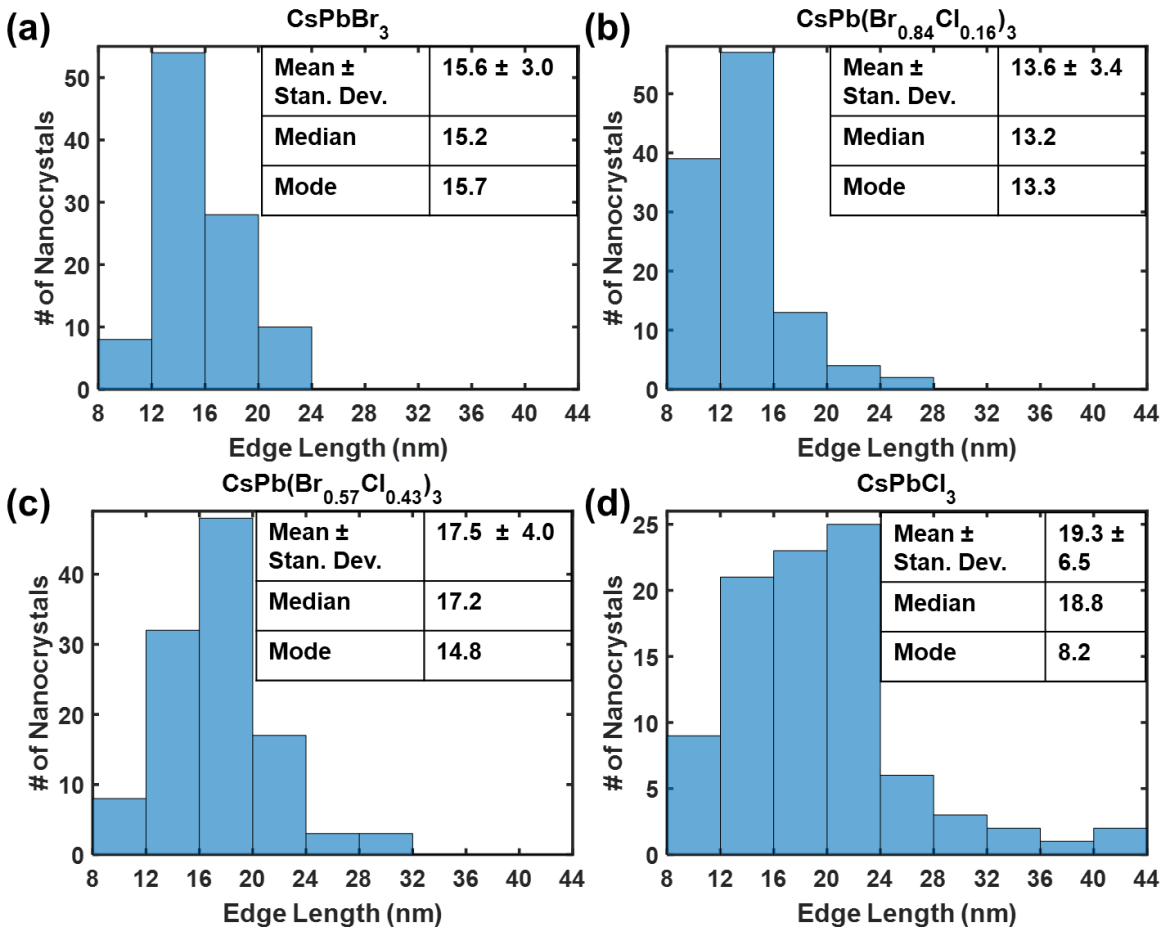

Figure S2: Edge-length-distributions of (a) $CsPbBr_3$, (b) $CsPb(Br_{0.84}Cl_{0.16})_3$, (c) $CsPb(Br_{0.55}Cl_{0.45})_3$, and (d) $CsPbCl_3$ NCs.

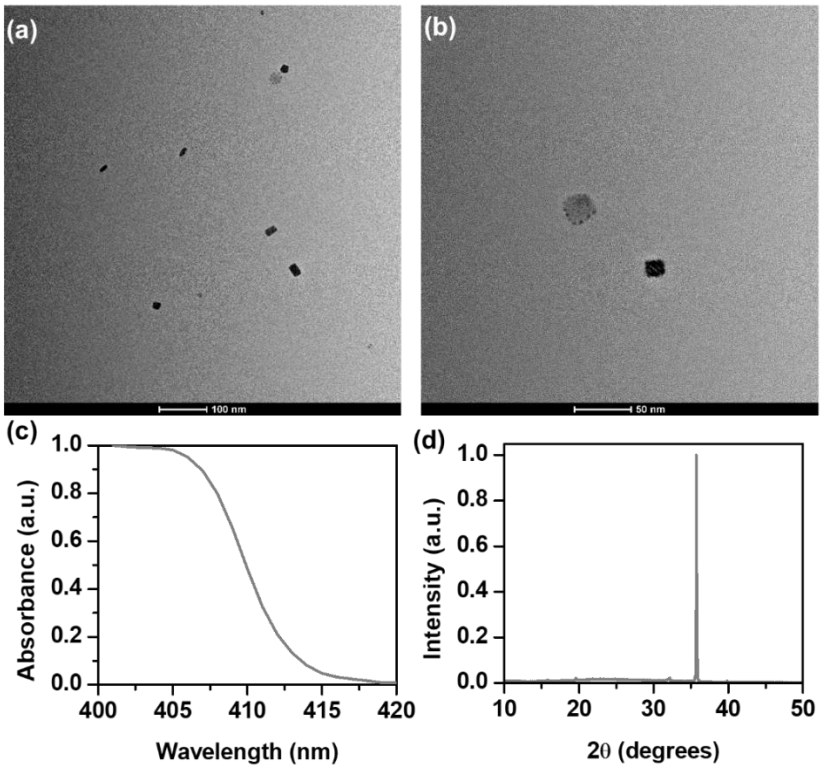

Figure S3: (a-b) TEM images, (c) absorbance spectrum, and (d) XRD spectrum of $CsPbCl_3$ NCs.

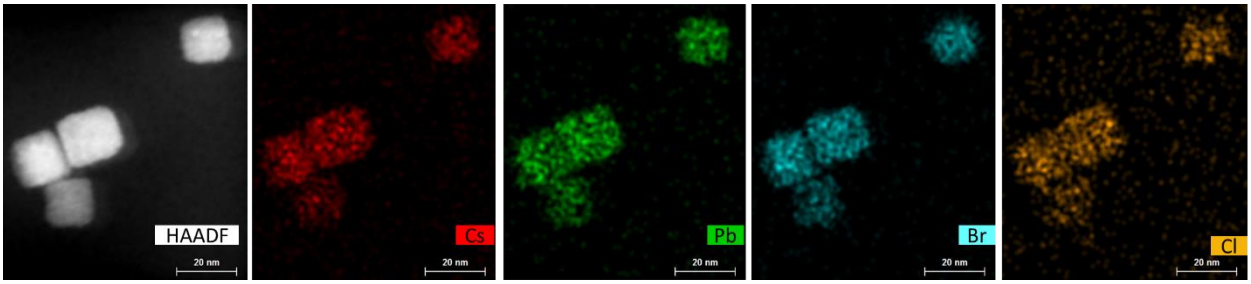

Figure S4: STEM-EDS maps of $CsPb(Br_{0.84}Cl_{0.16})_3$ Nanocrystals.

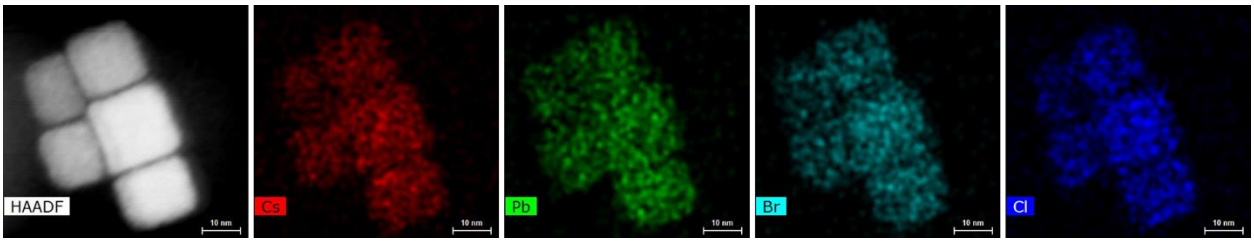

Figure S5: STEM-EDS maps of $CsPb(Br_{0.55}Cl_{0.45})_3$ Nanocrystals.

Table S2: Amplitudes (A_i) and lifetimes (τ_i) ± standard error (n = 4 samples per NC) and $\tau_{avg,}$ which is the amplitude-weighted lifetime of the different perovskite NC samples.

	Time-resolved Photoluminescence Spectroscopy						
	A_1	**τ_1 (ns)**	**A_2**	**τ_2 (ns)**	**A_3**	**τ_3 (ns)**	**τ_{avg} (ns)**
$CsPbBr_3$	0.59 ± 0.00	0.92 ± 0.08	0.34 ± 0.01	4.48 ± 0.11	0.08 ± 0.00	21.08 ± 0.83	3.66 ± 0.07
$CsPb(Br_{0.84}Cl_{0.16})_3$	0.66 ± 0.04	1.04 ± 0.12	0.25 ± 0.04	6.86 ± 0.95	0.09 ± 0.01	19.15 ± 1.15	3.67 ± 0.07
$CsPb(Br_{0.78}Cl_{0.22})_3$	0.78 ± 0.01	0.48 ± 0.02	0.20 ± 0.01	2.36 ± 0.04	0.02 ± 0.00	15.36 ± 0.69	1.19 ± 0.04
$CsPb(Br_{0.55}Cl_{0.45})_3$	0.87 ± 0.02	0.40 ± 0.02	0.12 ± 0.02	2.38 ± 0.24	0.01 ± 0.00	400.30 ± 192.58	0.70 ± 0.05

Table S3: Positions of the photobleach (PB), photoinduced absorption (PIA), and the bandgap renormalization energy (ΔE) at 6.5 µW. We observed that ΔE decreases at longer TA decay time with the exception of $CsPb(Br_{0.55}Cl_{0.45})_3$, in which case part of the PIA band was cut off since our white light probe only extends from 450 – 900 nm.

	Time (ps)	PB (nm)	PIA (nm)	ΔE_{rn} (eV)
$CsPbBr_3$	2	514	479	0.18
	20	514	488	0.13
	200	516	488	0.14
$CsPb(Br_{0.84}Cl_{0.16})_3$	2	495	469	0.14
	20	497	477	0.11
	200	497	477	0.11
$CsPb(Br_{0.78}Cl_{0.22})_3$	2	490	468	0.12
	20	490	469	0.11
	200	490	471	0.10
$CsPb(Br_{0.55}Cl_{0.45})_3$	2	460	-	-
	20	462		
	200	460		

Table S4: FWHM of the PB as a function of intensity per pulse and time. Note that for $CsPb(Br_{0.55}Cl_{0.45})_3$, the signal was too noisy at later times and weaker intensities to accurately determine the FWHM. Thus, the numbers provided for this sample are not a good reflection of the FWHM.

	Time (ps)	**Photobleach FWHM (nm)**		
		2.5 µW	**4.4 µW**	**6.5 µW**
$CsPbBr_3$	**10**	12.03	13.25	14.19
	40	12.02	12.51	12.73
	100	11.88	12.01	12.19
	200	11.28	11.28	11.76

$CsPb(Br_{0.84}Cl_{0.16})_3$	**10**	12.81	13.56	14.15
	40	11.79	12.43	12.08
	100	11.10	11.36	11.12
	200	10.69	10.67	10.53
$CsPb(Br_{0.78}Cl_{0.22})_3$	**10**	12.94	14.19	13.32
	40	11.89	12.94	12.22
	100	11.58	11.20	10.47
	200	10.56	11.69	9.73
$CsPb(Br_{0.55}Cl_{0.45})_3$	**10**	6.85	7.40	9.69
	40	5.77	5.52	7.12
	100	8.37	8.28	4.98
	200	3.68	6.36	5.55

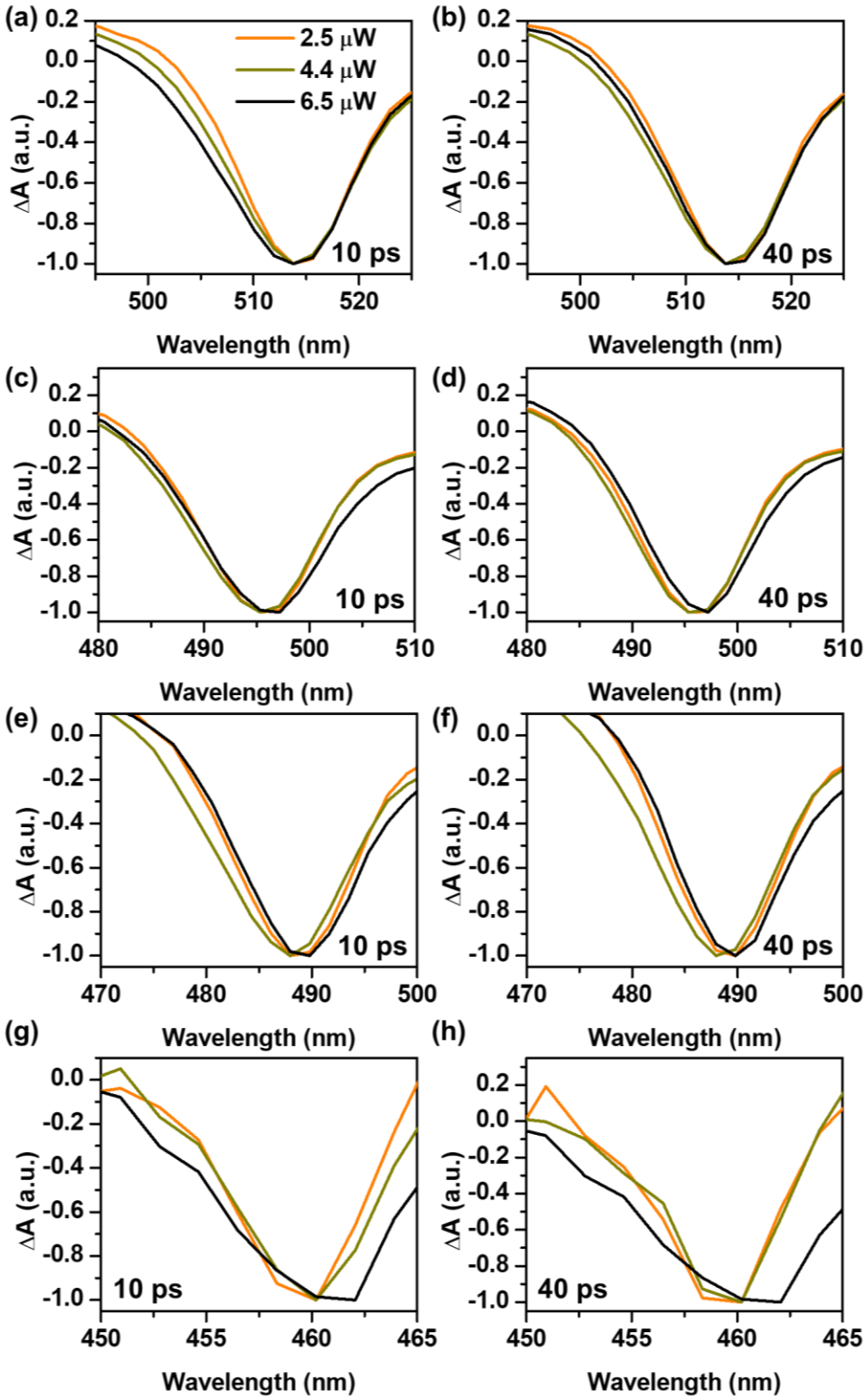

Figure S6: Evolutionary Spectra as a function of laser intensity at different delay times of (a-b) $CsPbBr_3$, (c-d) $CsPb(Br_{0.84}Cl_{0.16})_3$, (e-f) $CsPb(Br_{0.78}Cl_{0.22})_3$, and (g-h) $CsPb(Br_{0.55}Cl_{0.45})_3$.

Table S5: Parameters obtained from fits of the TA decays in Figure S7 ± the standard error or with the goodness of fit parameter, χ^2. The χ^2 values shown in the last column is obtained by fitting calculated values to experimentally obtained parameters by a nonlinear least-squares deconvolution method. Note that the formation of the PB in $CsPb(Br_{0.55}Cl_{0.45})_3$ was difficult to detect, leading to overestimated lifetimes at the lowest power.

	laser power (μW)	**τ_r (ps)**	**A_1**	**τ_1 (ps)**	**A_2**	**τ_2 (ps)**	**χ^2**
$CsPbBr_3$	**2.5**	0.19	0.35	472.03	0.61	460.07	0.12
	4.4	0.39	0.39	6.16	0.65	450.55	0.05
	6.5	0.60 ± 0.02	0.42 ± 0.01	5.9 ± 0.3	0.58 ± 0.01	831 ± 14	-
$CsPb(Br_{0.84}Cl_{0.16})_3$	**2.5**	0.28	0.26	20.34	0.74	309.89	0.03
	4.4	0.48	0.41	7.47	0.59	230.26	0.02
	6.5	0.41 ± 0.01	0.44 ± 0.02	34 ± 2.7	0.56 ± 0.02	333 ± 11	-
$CsPb(Br_{0.78}Cl_{0.22})_3$	**2.5**	0.12	0.20	55.62	0.80	411.95	0.11
	4.4	0.26	0.39	53.66	0.51	408.76	0.08
	6.5	0.32 ± 0.02	0.50 ± 0.03	34 ± 3.0	0.50 ± 0.03	397 ± 28	-
$CsPb(Br_{0.55}Cl_{0.45})_3$	**2.5**	0.33	0.66	15.07	0.34	261.81	0.20
	4.4	0.32	0.83	16.70	0.17	258.28	0.10
	6.5	0.33 ± 0.02	0.66 ± 0.08	14 ± 0.10	0.34 ± 0.08	150 ± 32	-

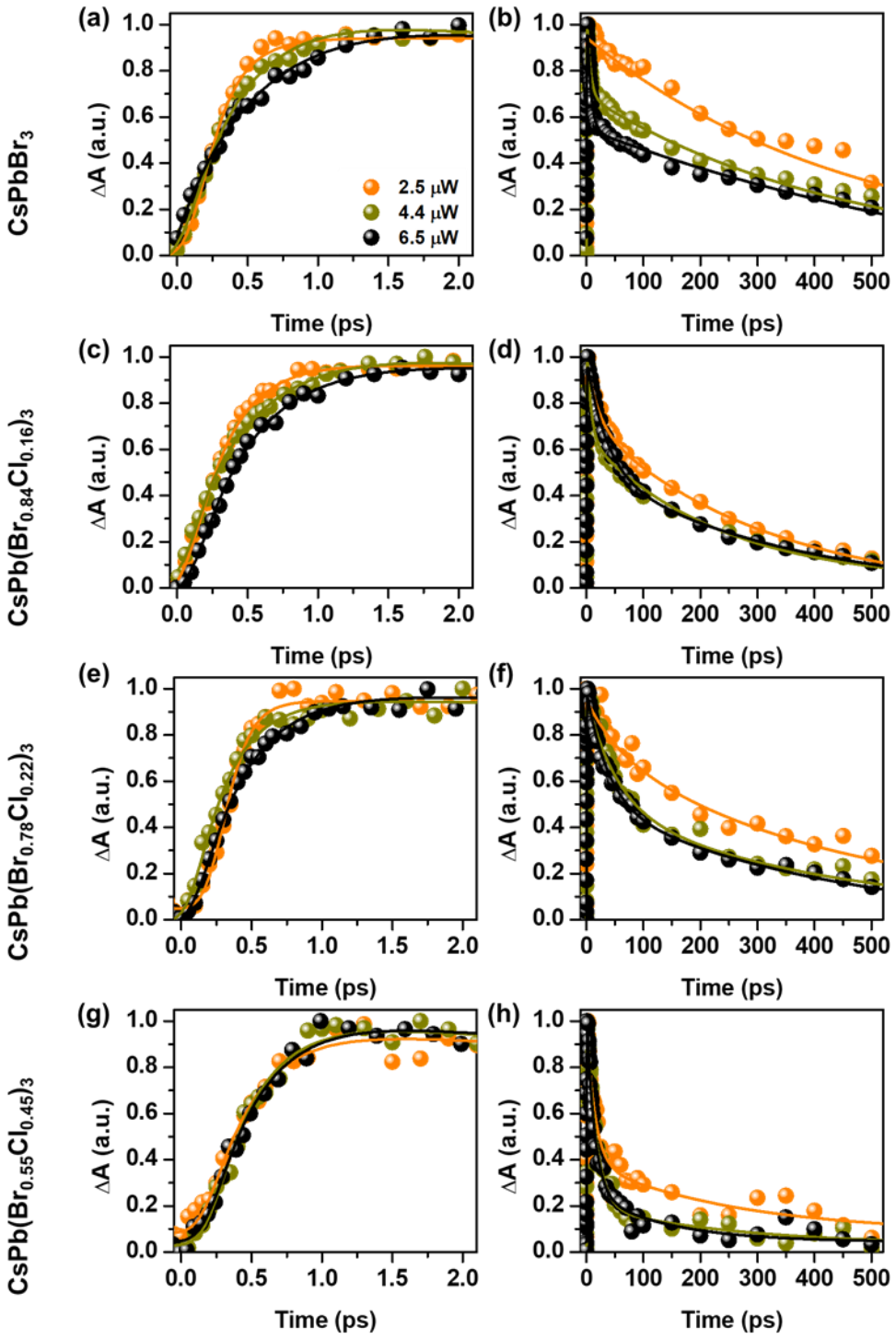

Figure S7: The formation and decay of the PB as a function of power for (a-b) $CsPbBr_3$, (c-d) $CsPb(Br_{0.84}Cl_{0.16})_3$ (e-f) $CsPb(Br_{0.78}Cl_{0.22})_3$, and (g-h) $CsPb(Br_{0.55}Cl_{0.45})_3$.

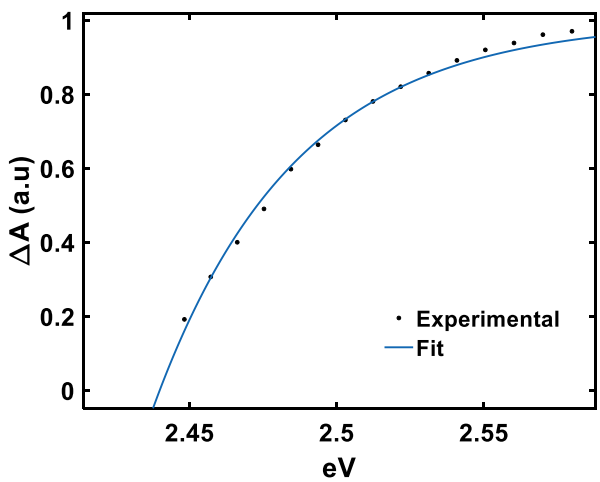

Figure S8: Plot showing how we estimated the carrier temperature by fitting the tail of the photoinduced absorption to a Boltzmann distribution. The plot shown is a fit of the high energy tail of the PB of $CsPbBr_3$ for one time point.

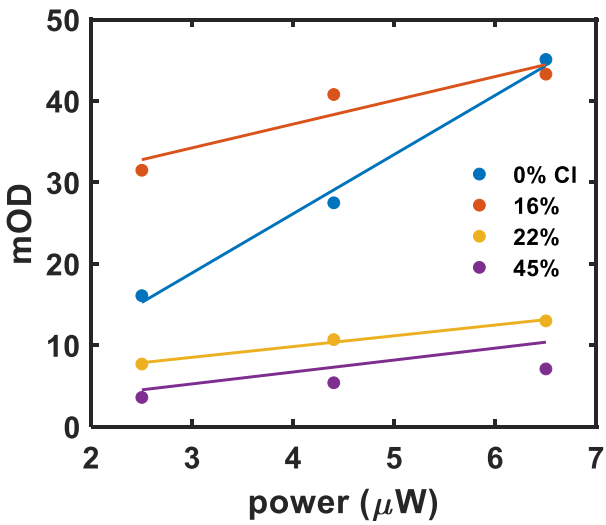

Figure S9: The photobleaching intensity as a function of pump fluence for the different NC samples show a linear slope indicative of Auger recombination. The parameters from the linear fits are provided in Table S5.

Table S6: Parameters of linear fit from Figure S10.

Sample	Slope	y-intercept	R^2
$CsPbBr_3$	7.2698	-2.9050	0.9912
$CsPb(Br_{0.84}Cl_{0.16})_3$	2.9192	25.4941	0.8824
$CsPb(Br_{0.78}Cl_{0.22})_3$	1.3210	4.5663	0.9890
$CsPb(Br_{0.55}Cl_{0.45})_3$	1.4634	0.8739	0.9979